GL04042

GEOTHERMAL EXPLORATION OF THE GRI LEASES IN BEAVER VALLEY, UTAH

Prepared for

GRI Operator Corporation
Menlo Park, California

by

Bruce S. Sibbett
Duncan Foley
Howard P. Ross

Earth Science Laboratory
University of Utah Research Institute
391 Chipeta Way, Suite C
Salt Lake City, Utah 84108
(801) 524-3422

CONTENTS

Page

EXECUTIVE SUMMARY....1

INTRODUCTION....3

GEOLOGY....5
- Introduction....5
- Regional Setting....5
- Lineament Analysis....6
- Structures....8
- Lithologies....12
- Alteration and Veins....14
- Age Dates....15

GEOCHEMISTRY OF SPRING WATERS....18
- Introduction....18
- Sampling Procedures....18
- Analytic Techniques....19
- Discussion of Results....19
- Comparison with Waters in Surrounding Areas....23

ELECTRICAL RESISTIVITY SURVEY....26
- Introduction....26
- Numerical Model Interpretation....27

COMPARISON OF GRI LEASE AREA WITH COVE FORT AND ROOSEVELT HOT SPRINGS KNOWN GEOTHERMAL RESOURCE AREAS (KGRAs)....35

RECOMMENDATIONS....37

REFERENCES CITED....39

APPENDIX I - NUMERICAL MODEL OUTPUT OF RESISTIVITY SURVEY....42

FIGURES AND PLATES

Page

Figure 1. Location map of GRI lease area....4

Figure 2. Lineament analysis of Beaver Valley to Cove Fort area....7

Figure 3. Simplified bedrock geology....10

Figure 4. Trilinear diagram of GRI lease area water samples,....22
selected thermal fluids, and cold waters.

Figure 5. Observed electrical resistivity data, dipole-dipole....28
line GRI-1.

Figure 6. Observed electrical resistivity data, dipole-dipole....29
line GRI-2.

Figure 7. Numerical model solution, line GRI-1....31

Figure 8. Numerical model solution, line GRI-2....32

Figure 9. Interpreted electrical resistivity distribution along....33
lines GRI-1 and GRI-2.

Plate I. Geologic map of the GRI lease block in Beaver Valley, Utah.

Plate II. Line location map, electrical resistivity survey, East
Mineral Mountains, Utah.

TABLES

1. Age Dates in the Roosevelt Hot Springs to Cove Fort Area....16

2. Limits of Quantitative Detection....20

3. Analytic Results and Chemical Geothermometry of Springs in....21
GRI lease area

4. Chemical Analyses Used for Trilinear Plots....24

EXECUTIVE SUMMARY

The Earth Science Laboratory/University of Utah Research Institute has evaluated selected lease holdings of GRI Operator Corporation in Beaver County, Utah, for the occurrence of geothermal resources. Geologic mapping, geochemical analyses of springs, and resistivity surveys failed to find any direct evidence of active geothermal systems, but the regional setting and geologic structures found during this study suggest that further exploration may be warranted.

The GRI geothermal leases in Beaver Valley encompass about nine and one-half square miles of primarily Tertiary igneous rock exposure between the Cove Fort and Roosevelt Hot Springs KGRAs. The western third of the lease area consists of syenite to gabbroic rocks of the Mineral Mountains intrusive complex. The plutonic rocks are overlain by Bullion Canyon Volcanics in the central part of the lease area. On the eastern one third of the lease area, 9 million year old rhyolites of Gillies Hill are down faulted against the Bullion Canyon Volcanics.

The lease area is located on a topographic high within the north-trending graben between the Tushar Mountains to the east and the Mineral Mountains to the west. North-south normal faults are the dominant structures within the study area.

Overall structural relief is down to the east, with the structurally lowest part of the Beaver Valley graben to the east of the lease area. Within the lease area, a narrow graben trends south-southeast from the syenite-Bullion Canyon Volcanics contact, across the Bullion Canyon Volcanics to the Gilles Hill rhyolite in the central lease area. Abundant quartz veins,

felsite dikes and alteration occur along this graben. Just west of the lease, Quaternary basalt flows and two cinder cones cover a mile-wide, north-trending graben.

Geochemical analyses of spring waters from the study area show normal ground water without any clear indication of a thermal component. Springs within this topographically high area come from local recharge and have not traveled to significant depths.

Two dipole-dipole resistivity lines, totaling 5.3 line miles within the study area, found no major anomalous low resistivity zones within 2500 feet of the surface. A narrow zone of 25 ohm-m rock near Station 0 on Line 2 may indicate alteration along structures. Major resistivity boundaries are in excellent agreement with surface mapped faults. The numerical model results for Line 2 indicate a more complex series of vertical structures along the western edge of the graben.

Further electrical survey work and thermal gradient studies are the next exploration techniques that should be applied toward defining any geothermal systems that might exist at depth. A reconnaissance bipole-dipole survey to explore to greater depths and test structures in the northeast part of the lease area is recommended as one step to evaluate further the area. Thermal gradient drilling, particularly in the most promising structural target areas of the northeast part of the lease block, could demonstrate any anomalies.

INTRODUCTION

The GRI lease area consists of 6,219 acres in northern Beaver County, situated in a hilly area midway between the Cove Fort and Roosevelt Hot Springs high-temperature geothermal systems (Fig. 1). Twenty megawatts are currently being produced at Roosevelt Hot Springs, and 2.8 MW wellhead generators are being installed at the dry-steam field at Cove Fort (DiPippo, 1984).

Detailed geologic mapping, water sampling from springs and a dipole-dipole electrical resistivity survey were carried out in the lease area to identify and evaluate lithologies and structures which may be favorable for the occurrence of a geothermal resource. This exploration program provides data to facilitate planning and decisions on further exploration efforts.

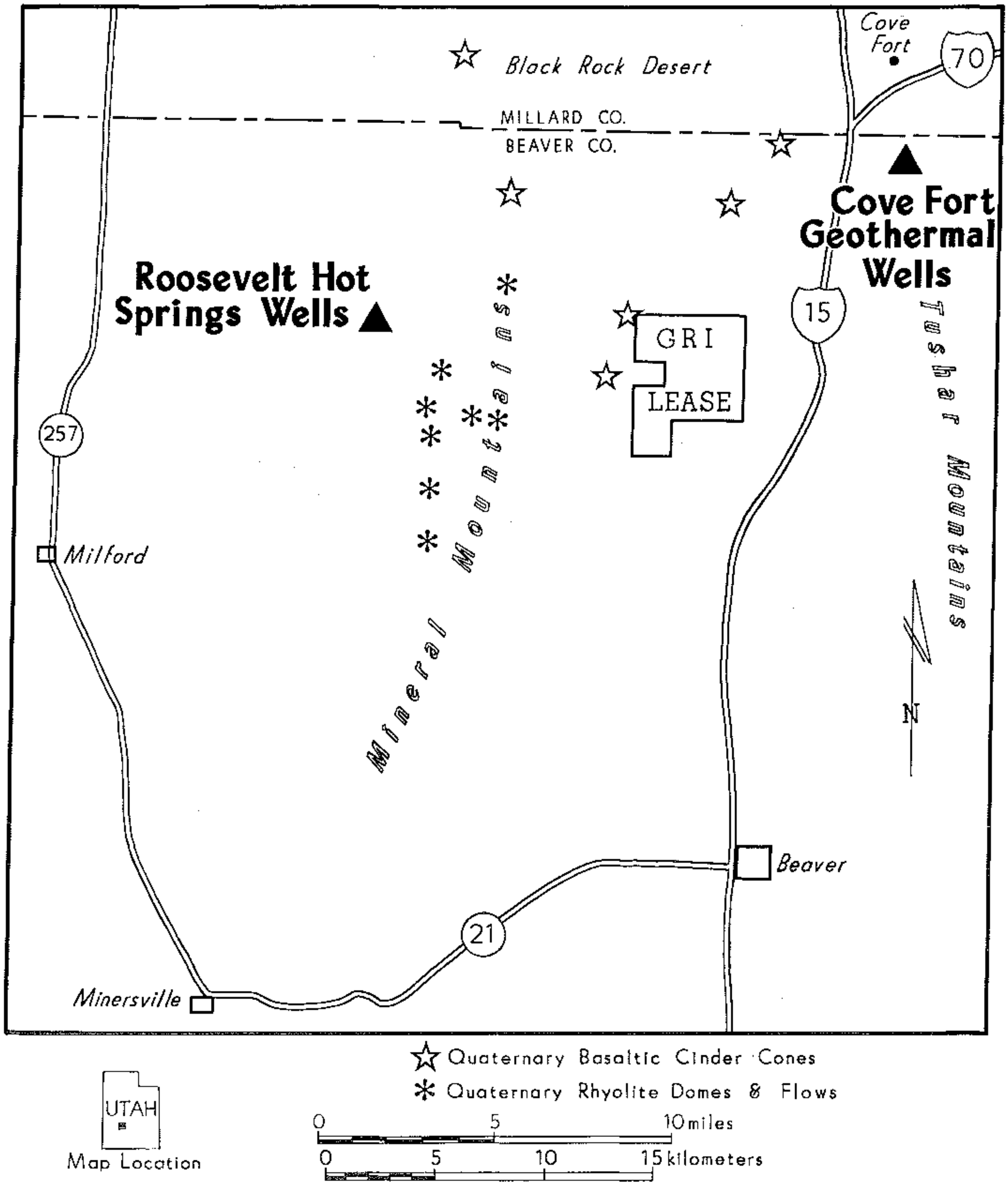

Figure 1. Location map of GRI Lease area, Roosevelt Hot Springs and Cove Fort geothermal areas.

GEOLOGY

Introduction

The most detailed previously existing geologic map of the GRI lease area is by Machette and Steven (1983). This map emphasizes Tertiary and Quaternary alluvial and lacustrine stratigraphy; bedrock stratigraphy and structures depicted on the GRI lease area have been significantly refined by us on the geologic map (Plate I) included in this report. Particular attention was paid in this study to defining structures which may control possible geothermal fluids at depth in the GRI lease area.

Regional Setting

The GRI lease is located near the eastern edge of the Basin and Range geologic province, which is characterized by north-trending horsts and grabens bounded by normal faults. The lease area is in the east-west-trending Wah Wah-Tushar mineral belt (Mabey et al., 1978), which has been the site of intrusive activity through the Tertiary and into Quaternary time. The Mineral Mountains to the west are a structural high relative to adjacent ranges (Ross et al., 1982a). In the Cove Fort area to the east, Tertiary volcanic rocks of the Marysvale volcanic field overlie Paleozoic- to Mesozoic-age sedimentary rocks (Moore and Samberg, 1979). Quaternary rhyolitic volcanism has formed lava flows, domes and ash-flows in the Mineral Mountains. Basalt flows cover much of the valley north of the lease area. Deep normal faults seem to control the geothermal systems at both Roosevelt Hot Springs and Cove Fort. Low-angle faults provide reservoir fracture systems or other control in the production zone at Roosevelt and Cove Fort (Nielson and Moore, 1979).

Lineament Analysis

Landsat imagery was examined and lineaments were plotted for the Beaver Valley-Cove Fort area. This lineament analysis was carried out to identify possible regional structures which are not apparent in the limited area mapped in detail and to give an indication of the setting of the study area relative to the Roosevelt and Cove Fort areas. Non-cultural linears on small scale imagery such as Landsat are generally formed by topographic, vegetative or soil color changes. Topographic linears may be formed by aligned drainages, escarpments or ridge lines that are controlled by differential erosion along rock changes, faults and joint concentrations. Vegetative linears are formed by a change in plant vigor or plant type due to abundance of moisture or soil type. Variation in soil moisture has a greater effect than soil type and may be due to change in elevation, direction of slope exposure or hydrologic character of the subsurface. All the vegetative changes evident on the Landsat imagery examined in this study were due to elevation or slope exposure orientation and therefore were not mapped.

All but one of the linears shown on Figure 2 have a topographic expression. The east-northeast-trending linear ("A" on Fig. 2) south of the GRI lease area is a change in soil color (possibly vegetative cover) from darker on the north to lighter on the south. The linear trends across the south to southeast drainage system in the area and appears to correlate with northeast-trending linears in the bedrock of the Tushars to the east.

Overall, the linears define a north-trending structure (graben?) between the Mineral Mountains and the Tushars. Note that east-west linears such as the Negro Mag fault on the west and the linears in the Tushar Mountains splay out toward the graben and appear to be truncated by it (Fig. 2). The best

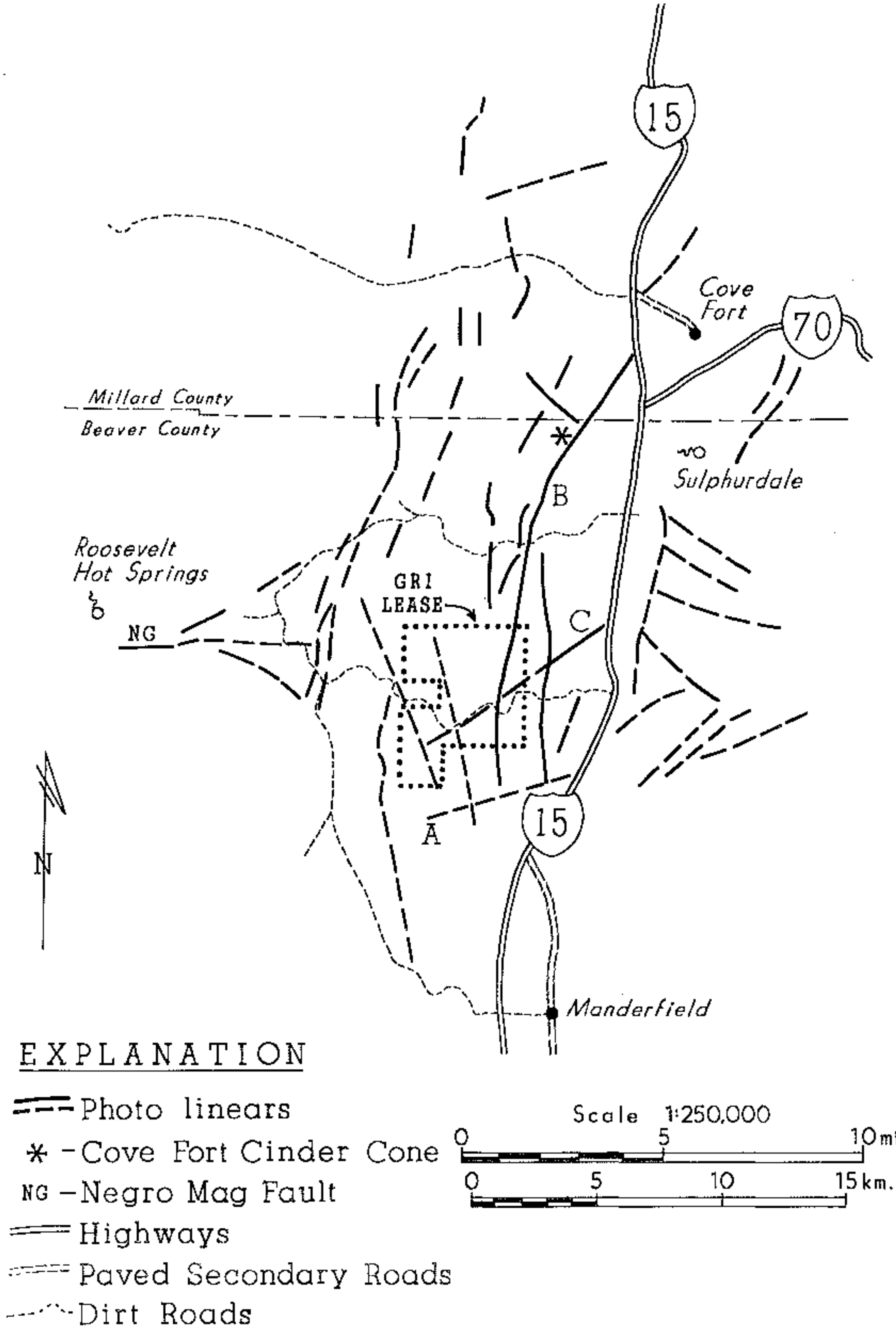

Figure 2. Lineament analysis of Beaver Valley to Cove Fort area.

defined linear is formed by the recent fault that offsets the Cove Fort cinder cone and extends south to the escarpment on the west side of the Fourmile Ridge ("B" on Fig. 2; Plate I). This linear extends south along the small graben separating the Gillies Hill rhyolite from the Bullion Canyon Volcanics. Small sagpond depressions along the east fault of the graben suggest that recent movement has occurred in the southeast part of the study area. Recent movement has been down to the west along the entire length of the linear.

One other noteworthy linear is the northeast-trending linear in the lease area ("C" on Fig. 2). Although a structure was not found in the field in this location, several dikes, veins, faults and drainages follow this trend (Plate I). The linear follows the drainage next to which resistivity Line 2 was run, passes near Fourmile Spring, part of Bull Hollow and near Woodtick Hill (Plate I) east of the lease area. Mapped faults following this northeast trend, just to the north of the Landsat linear, could be interpreted as having a left lateral component of offset (Plate I, see Structures section below). Offset of a dike across the Negro Mag fault in the Roosevelt Hot Springs KGRA could also be interpreted as left lateral (Nielson et al., 1978).

Structures

The dominance of north-south structures controlling the general distribution of lithologies in the study area is evident on Plate I. The largest of these structures is a mile wide graben capped by the Quaternary basalt flow (Qb), just west of the GRI lease area (Plate I). The graben bounds the west side of Paleozoic quartzite (Pzq) and the syenite (Ts). The graben faults seem to have provided the channel way for the basaltic volcanism which formed Crater Knoll and Red Knoll cinder cones. These two vents and a normal fault in Section 36, T26S, R8W are along a north-northeast trend which continues through the younger cinder cones near Cove Fort. A north-northwest fault trend which offsets the basalt flow south of Crater Knoll continues into the fault and dike system which bounds the east side of the Mineral Mountains to the northwest (Sibbett and Nielson, 1980; Plate I of this paper is included as part of the age date compilation maps). Crater Knoll is situated at the intersection of the north-northwest and north-northeast structural trends.

A narrow graben, one thousand feet wide or less, is present at the fault boundary between the Bullion Canyon Volcanics and the Gilles Hill rhyolite, west of Gillies Hill (Fig. 3 and Plate I). Small fault sag areas along the east side of the graben are evident on aerial photographs suggesting recent movement along this fault. West of Fourmile Spring the graben system appears to be displaced 2000 feet west and trends north-northwest across the Bullion Canyon Volcanics to the contact with the syenite in Section 31, T26S, R7W (Fig. 3). Rocks within the graben are poorly exposed and hematite stained to argillically altered. Therefore, correlation with Gillies Hill rhyolite is somewhat uncertain. The rock is generally light colored with very few phenocrysts, as are Gillies Hill rocks.

The fault bounding the west side of Fourmile Ridge, in the northeast corner of the study area, appears to have a noticeable scarp on aerial photographs. This fault is on line with the recently active fault to the south, west of Gillies Hill. No direct connection could be found on the ground or on aerial photographs, however a linear on Landsat images is continuous along these faults.

Another north-trending fault system is present on the east side of Gillies Hill. Parts of these faults were mapped where they cross Bull Hollow,

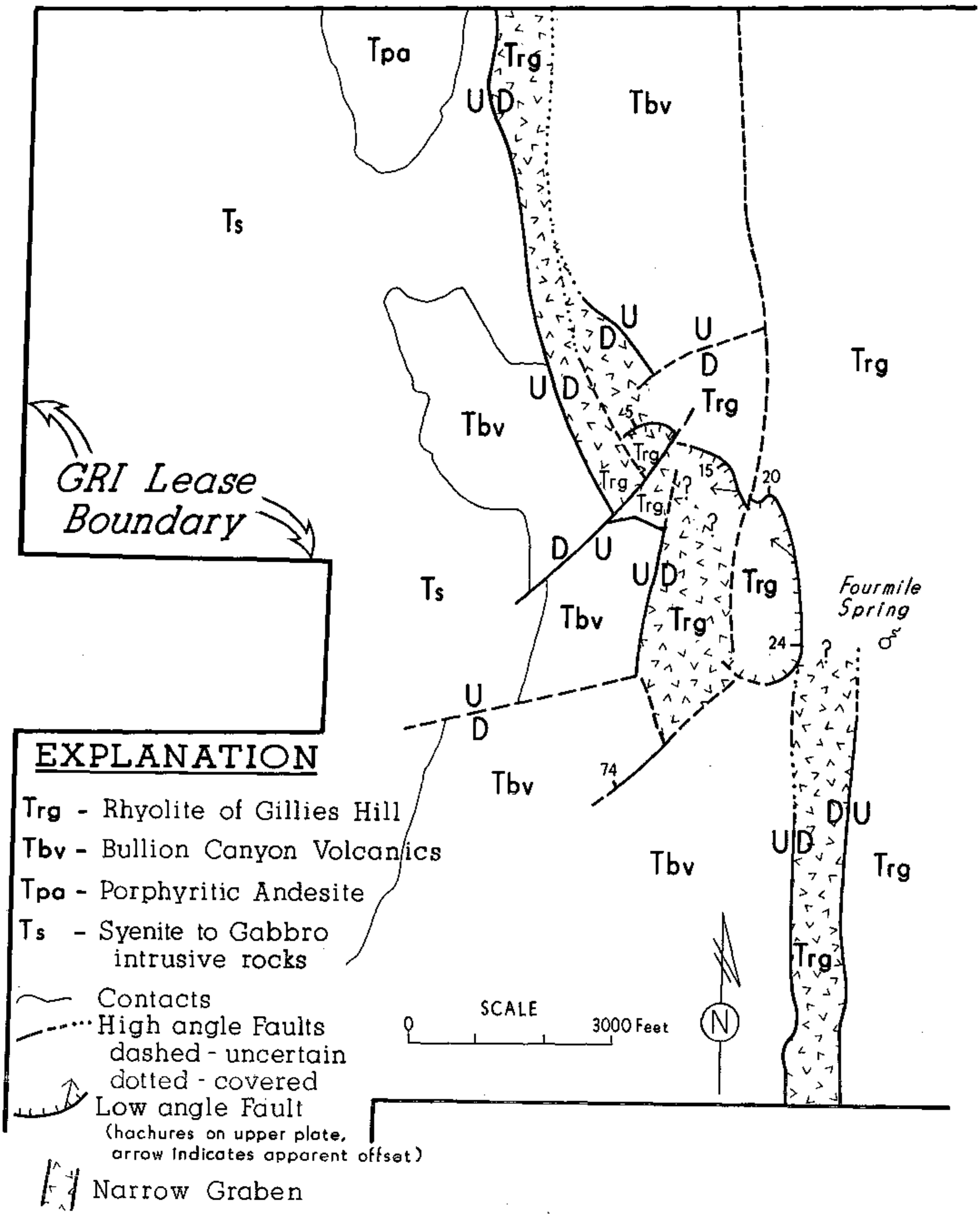

Figure 3 Simplified bedrock geology showing major lithologic and structural units.

just east of the lease area (Plate I).

A lower-angle fault, with a 20-foot thick breccia zone exposed, is present near the top of the small hill 1300 feet west of Fourmile Spring. Slickenside surfaces within the fault breccia dip 15 to 24 degrees to the northwest (Plate I and Fig. 3). Striations or groves are nearly parallel with the dip direction. Extensive quartz veins within the fault make up a large part of the breccia in places, indicating more than one movement along the low-angle fault. The extent of this low-angle faulting is unknown, but it may have formed by sliding of rhyolite into the small graben west of the fault. A fault surface dipping 9° southwest caps a small hill 3600 feet southwest of Fourmile Spring, on the west edge of the graben.

A secondary structural trend in the study area is east-northeast. Many of the felsite dikes (Tif), the porphyritic rhyolite dike (Tpr) and several mapped faults follow this trend.

Overall, the structures in the study area have exposed older or deeper rocks to the west and younger Tertiary rocks to the east. Therefore, net offset is down to the east. The model interpretation of resistivity line 2 is in close agreement with this interpretation. Measured dips on bedded units are too sparse and diverse to indicate any regional tilting.

As mentioned above, the pluton-sedimentary rock contact on the southeast side of the Mineral Mountains projects into the west side of the GRI lease block. The uplift of the Mineral Mountains pluton (Evans and Nielson, 1982) fits with the up-to-the-west structural setting of the study area. The thrust fault exposed to the southwest (Sibbett and Nielson, 1980) was not found in the study area. Judging by the metamorphosed condition of the Paleozoic rocks and proximity to plutonic rocks, the Paleozoic rocks are probably part of the lower plate. The thrust, therefore, probably is not present in the lease block.

The structures in the study area most likely to carry geothermal fluids at depth would be the faults bounding the graben under Crater Knoll, which is west of the GRI leases, and the narrow graben in the north-central part of the lease area. No evidence of recent hot springs activity or recent alteration was found along either of these structures, however. The lease area may serve as a recharge area due to the high topographic and hydrologic setting.

Lithologies

Paleozoic quartzite and meta-carbonate rocks, the oldest formations in the area, crop out along two north-trending exposures in the southwest part of the lease area (Plate 1). These Paleozoic rocks are intruded by the syenite (Ts), a quartz-rich leucocratic granite (Tg) and felsic rhyolite dikes (Tif). The quartz-rich granite is the same unit which forms the east edge of the Mineral Mountains pluton exposed two miles west of the GRI lease block. The intrusive contact between granite and quartzite on the east edge of the Mineral Mountains pluton is exposed four miles to the southwest and this contact trends northeast (Sibbett and Nielson, 1980; Plate I enclosed), projecting directly to the west side of the GRI lease area. As in the lease area, carbonate rocks are exposed to the east of the quartzite along the southeast margin of the pluton. However, there is a phyllite unit present between the quartzite and the overlying carbonates in the Mineral Mountains. The phyllite, if present in the study area, would be under the colluvium (QTs) which covers Cherry Hollow between the quartzite and carbonate exposures. Correlation of the granite, quartzite and carbonate along the margin of the pluton suggests that the GRI lease area is along the east margin of the Mineral Mountains pluton.

The Tertiary phaneritic intrusive rocks in the study area are probably phases of the Mineral Mountains intrusive complex. As mentioned above, the quartz-rich granite is one of the major phases of the intrusive complex. The syenite in the Roosevelt KGRA is much coarser grained and more leucocratic (Sibbett and Nielson, 1980) than the syenite in the study area. However, the syenite and monzonite to diorite lithologies in the study area all have counterparts in the intrusive complex (Sibbett and Nielson, 1980). The plagioclase-rich gabbro (Tig) in the study area is probably also a mafic phase of the Mineral Mountains intrusive complex, and the gabbro may grade to diorite, depending on the anorthite content of the plagioclase. The age of the gabbro relative to the syenite is uncertain, but the gabbro is less altered and may therefore be younger than the sheared and weakly altered syenite.

The Bullion Canyon Volcanics are a heterogeneous assemblage of intermediate composition, generally porphyritic lava flows, ash-flow tuffs and water-lain pyroclastics. The relative ages of the Bullion Canyon Volcanics and the syenite and gabbro are not clearly demonstrated in the GRI lease area. Sparse radiometric data on the Mineral Mountains intrusive complex (Evans and Nielson, 1982) and ages assigned to the Bullion Canyon Volcanics (Machette and Steven, 1983; Rowley et al., 1979) suggest that the older, more mafic phases of the intrusive complex are of similar age to the Bullion Canyon Volcanics. The granitic phases are younger (Evans and Nielson, 1982) than the Bullion Canyon Volcanics, however.

The Gillies Hill rhyolite lava flows and ash-flow tuffs overlie the older volcanic rocks, although they are in fault contact in the lease area. The felsite dikes cut all older units in the study area but do not intrude the 9 m.y. old Gillies Hill rhyolites (Machette and Steven, 1983) except possibly in the graben along the west side of Gillies Hill. The felsite dikes are lithologically similar to the Gilles Hill rhyolites and may be vents for some of the surface flows. Quartz veins are present within or along many of the felsite dikes and there seems to be a direct association. The porphyritic rhyolite dikes (Tpr) are similar to the extensive dikes to the northwest of the lease block which intrude the Mineral Mountains pluton.

Colluvium and fanglomerates with intercalated lacustrine clay (QTs) cap old piedmont surfaces in the southern part of the lease area. These deposits were correlated by Machette and Steven (1983) with Pliocene to Pleistocene lake events in the Beaver Valley.

Alteration and Veins

Significant alteration is restricted to the narrow, north-trending graben in the north-central part of the lease area, a small area around Cowboy Springs, a small area in the NE 1/4, Sec. 1, T27S, R8W (Plate I) and in the area east of Fortuna Canyon, north of the Fortuna mine. Alteration in these areas consists of propylitic to moderate argillic assemblages. Silicification of felsite dikes and fault breccias has occurred at many locations in these areas of alteration. The quartz veins are generally barren of box-works or strong iron staining. However, mining activity has occurred along iron-stained quartz veins associated with the narrow graben in Section 6 and 7, T27S, R7W. These are possibly gold occurrences. The northern third of the lease area is covered with active mining claims. All of the alteration and quartz veining appear to be old and no indication of recent hydrothermal activity was found.

Age Dates

Published age dates for 18 rock samples from the Mineral Mountains and Cove Fort area are tabulated in Table 1 and plotted on the accompanying topographic maps. The Quaternary rhyolite lava flows, domes and ash flows in the Mineral Mountains range in age from 0.79 ± 0.08 m.y. to 0.50 ± 0.07 m.y. (Lipman et al., 1978). The GRI lease position is about as close to these young rhyolites as is Roosevelt Hot Springs (Fig. 1). Available age dates for phases of the Mineral Mountains intrusive complex vary widely but three are listed in Table 1 (Evans and Nielson, 1982). These are K-Ar dates and later thermal events have reset or partly reset most Tertiary K-Ar dates in the range. Age studies using rubidium-strontium and U-Pb techniques (Aleinikoff et al., in press) indicate phases of the pluton range from 27 m.y. to younger than 12 m.y. (Evans and Nielson, 1982).

The basalt flow associated with Crater Knoll, three-fourths mile west of the GRI lease area, is dated at 1.0 ± 0.3 m.y. (Best et al., 1980). A sample from the basalt capping Black Mountain (on the Beaver SW 7-1/2 minute quadrangle) 5 miles to the south of the lease area was dated as 1.1 ± 0.3 m.y. (Best et al., 1980). This is probably the same lava flow which flowed south from Crater Knoll, although alluvium covers the connection between the basalt exposures. The basalt flow that issued from Red Knoll, at the northwest corner of the lease area, has not been dated, but the degree of weathering and geomorphic expression suggest that the flow is about the same age as the Crater Knoll flow, about one million years old.

The Gillies Hill rhyolite has been dated at about 9.1 m.y. (Evans and Steven, 1982). These are the youngest silicic rocks exposed in the lease area. The two discordant age dates on Gillies Hill rhyolite, 6.96 m.y. and

TABLE 1

AGE DATES IN THE ROOSEVELT HOT SPRINGS TO COVE FORT AREA

Unit and Lithology	Location (Lat. N, Long. W)	Age (m.y. ± 2σ)	Reference
Bailey Ridge, Obsidian	38°29',112°49'	0.79 ± 0.08	Lipman et al., 1978
Ranch Ridge, Obsidian	38°25',112°50'	0.70 ± 0.04	Lipman et al., 1978
So. Twin Flat Mtn., Sanidine	38°25', 112°49'	0.50 ± 0.07	Lipman et al., 1978
Bearskin Mtn. Dome, Obsidian	38°27', 112°47'	0.60 ± 0.12	Lipman et al., 1978
North Dome, Sanidine	38°31', 112°47'	0.54 ± 0.06	Lipman et al., 1978
Little Bearskin Dome, Sanidine	38°27', 112°48'	0.61 ± 0.05	Lipman et al., 1978
Corral Canyon Dome, Biotite	38°24', 112°53'	7.90 ± 0.30	Lipman et al., 1978
Biotite Granite, Tbg	38°24'30", 112°50'	11.8 ± 0.6	Evans & Nielson, 1982
Hornblende Diorite, hd	38°35', 112°50'30"	27.2 ± 0.9	Evans & Nielson, 1982
Quartz Monzonite, Tqm	38°34', 112°50'45"	12.1 ± 0.5	Evans & Nielson, 1982
Cove Fort Andesite Flow	38°32'25", 112°41'25"	0.3 ± 0.1	Best et al., 1980
Basalt Flow, Qbm	38°22'18", 112°42'13"	1.1 ± 0.3	Best et al., 1980
Basalt Flow, Qb	38°26'21", 112°44'11"	1.0 ± 0.3	Best et al., 1980
Basalt Flow	38°37'33", 112°40'18"	0.5 ± 0.1	Best et al., 1980
Rhyolite Dome	38°28'26", 112°38'53"	6.96 ± 0.35	Evans & Steven, 1982
Rhyolite Dome	38°30'32", 112°38'13"	9.22 ± 0.46	Evans & Steven, 1982
Rhyolite Dome	38°31'46", 112°38'34"	8.01 ± 0.32	Evans & Steven, 1982
Rhyolite Dome	38°32'1", 112°37'56"	9.11 ± 0.64	Evans & Steven, 1982

8.01 m.y., are due to argon loss from partly oxidized biotite (Evans and Steven, 1982).

Two age dates have been obtained for basalt flows associated with Cinder Crater, 5 miles north of the lease area. One of these is the youngest date for exposed rocks in the Cove Fort area at 0.3 ± 0.1 m.y. (Best et al., 1980) for a basalt flow 3 miles north of the lease area. Examination of aerial photographs indicates this flow issued from the Cinder Crater vent area and overlaps the older flow which flowed north from Red Knoll. Quaternary rhyolite is not exposed in the Cove Fort area.

The youngest rhyolite dome at Twin Peaks, 20 miles northwest of the study area, is 2.35 ± 0.08 m.y.; the youngest basalt has been dated at 0.97 ± 0.25 m.y. (Crecraft et al., 1981). Other rhyolite and basalt units of similar age are present in the Twin Peaks and Black Rock Desert volcanic field (Hoover, 1974).

Bimodal volcanism is typical of Late Tertiary to Quaternary igneous activity in the Basin and Range Province (Rowley et al., 1979). The rhyolites in the Mineral Mountains and the basalts extending from the northern part of the range to Cove Fort may be the two components of a single volcanic field. The GRI lease area appears to be on the east edge of this volcanic field.

GEOCHEMISTRY OF SPRING WATERS

Introduction

Geochemical constituents in water can sometimes be interpreted to indicate the presence of thermal fluids at depth, even in areas where the thermal waters are mixed with cooler fluids at the surface. In the lease area, a limited program of water sampling was undertaken to seek direct or indirect evidence for the existence of thermal fluids at depth.

No thermal springs were found in the lease area. All waters sampled were 8°C or cooler. No thermal spring deposits were identified, and no evidence for geologically young zones of hydrothermal alteration was found.

Five of the six sampled springs are identified on Plate I. The sixth, Willow Spring, is identified on Plate I of the Geology of the Central Mineral Mountains (Sibbett and Nielson, 1980), a copy of which is included with this report.

Sampling Procedures

Water samples were collected following the techniques of Kroneman (1981). Three water samples were collected at each spring. All were pressure filtered through a 45 μ filter. A 60 ml sample was diluted with 20% HNO_3 for ICPQ analysis, a 500 ml sample was treated with 1% HCl for SO_4 analysis, and a filtered, untreated sample was collected for the remaining analyses. Temperature was measured with a Taylor dial thermometer, and pH was measured at the time of sample collection with a Lamotte pH meter (Model HA). The air temperature at the time of sample collection was approximately 0°C. Flow rates for the springs were measured or estimated for five of the sites. Flow was too diffuse, with too many outlets over too large an area, for a reliable estimate to be made at "Burnt Oak Spring"; flow here is probably tens of liters per minute.

Analytic Techniques

All analyses were performed at the Earth Science Laboratory. Cations were measured on an ARL Inductively Coupled Plasma Quantometer (ICPQ). Table 2 lists the limits of quantitative detection for ICPQ analyses of waters. HCO_3 and Cl were titrated in the laboratory. SO_4 and TDS were measured by gravimetric methods, TDS values were calculated following the method of Hem (1970), and F was measured with a specific ion electrode.

Discussion of Results

Table 3 presents the results of the analyses of the waters sampled in the GRI study area. The chemical characteristics of these waters do not indicate that they have ever been heated to a high temperature, or that a high temperature water has mixed with the local cool groundwater. The sampled waters have relatively low silica concentrations, low total dissolved solids, and are primarily Ca-HCO_3 in composition.

Chemically, most of the waters are similar. Figure 4 is a trilinear plot of the waters analyzed during this study. Wiregrass Spring (#5) is unusual, in having slightly lower TDS. It was collected, however, immediately below a cattle pond, and may represent seepage through the dam rather than the original spring that was impounded at the site. Willow Spring (#6) flows from quartz monzonite, which probably accounts for the higher level of fluoride.

Chemical geothermometers calculated from these analytic results are also presented in Table 3. These geothermometers also suggest that the waters do not have a high-temperature thermal history. The highest cation geothermo-

TABLE 2

LIMITS OF QUANTITATIVE DETECTION[1]

Analytical Method		Detection Limits (ppm)
ICP	Na	0.61
	K	1.22
	Ca	0.24
	Mg	0.49
	Fe	0.02
	Al	0.61
	SiO_2	0.52
	B	0.12
	Li	0.05
	Sr	0.01
	Zn	0.12
	Ag	0.05
	As	0.61
	Au	0.10
	Ba	0.61
	Be	0.01
	Bi	2.44
	Cd	0.06
	Ce	0.24
	Co	0.02
	Cr	0.05
	Cu	0.06
	La	0.12
	Mn	0.24
	Mo	1.22
	Ni	0.12
	Pb	0.24
	Sn	0.12
	Sb	0.73
	Te	1.22
	Th	2.44
	Ti	0.12
	U	6.10
	V	1.22
	W	0.12
	Zr	0.12
Titrimetric	Total Alkalinity as HCO_3	10.00
Gravimetric	SO_4	2.00
Titrimetric	Cl	2.00
ICP	PO_4	1.84
Specific Ion Electrode	F	0.10
Gravimetric	Total Dissolved Solids	4.00

[1] Limit of quantitative detection is the concentration in natural waters at which the analytic precision is ± 100%, with a confidence level of 95%.

TABLE 3

ANALYTIC RESULTS AND CHEMICAL GEOTHERMOMETRY OF SPRINGS IN GRI LEASE AREA[1,2]

Sample	Fourmile Spg	Cowboy Spg	Burnt Oak Spg	Live Oak Spg	Wiregrass Spg	Willow Spg
Temperature (°C)	8	5.5	5.5	5	6	5
pH	6.4	6.6	7.5	6.8	6.5	7.4
Na	15	40	25	28	8.5	36
K	2	2	2.2	13	2.5	4.4
Ca	49	105	114	96	34	64
Mg	11	31	29	27	8	14
SiO_2	27	19	19	22	24	38
Sr	0.2	0.4	0.5	0.5	0.2	0.3
Zn	nd	0.15	nd	nd	0.2	nd
HCO_3	97	350	322	310	121	289
SO_4	15	43	60	52	10	19
Cl	77	90	92	109	21	34
F	nd	0.2	0.2	nd	0.2	0.8
TDS meas.	262	516	490	518	156	323
calc.	244	503	501	499	168	352
cation/anion (%)	0.02	2	0.6	4.1	0.3	0.8
Geothermometers (°C)						
Quartz (no steam)[3]	75	62	62	68	70	89
Chalcedony[3]	43	30	30	36	38	58
Na-K-Ca[4]	17	14	12	59	25	40
Flow rate (l/m)	8.2	12.5	diffuse	10 (est.)	5 (est.)	20 (est.)

1. Concentrations in ppm (nd = not detectable).

2. Elements analyzed for but not present above the limits of quantitative detection include Fe, Al, B, Li, Ag, As, Au, Ba, Be, Bi, Cd, Ce, Co, Cr, Cu, La, Mn, Mo, Ni, Pb, Sn, Sb, Te, Th, Ti, U, V, W, Zr.

3. Calculated from formulas of Fournier (1981).

4. Calculated from formulas of Fournier and Truesdell (1974). No Mg corrections applied as all Na-K-Ca calculated tempratures are less than 70° (Fournier and Potter, 1979).

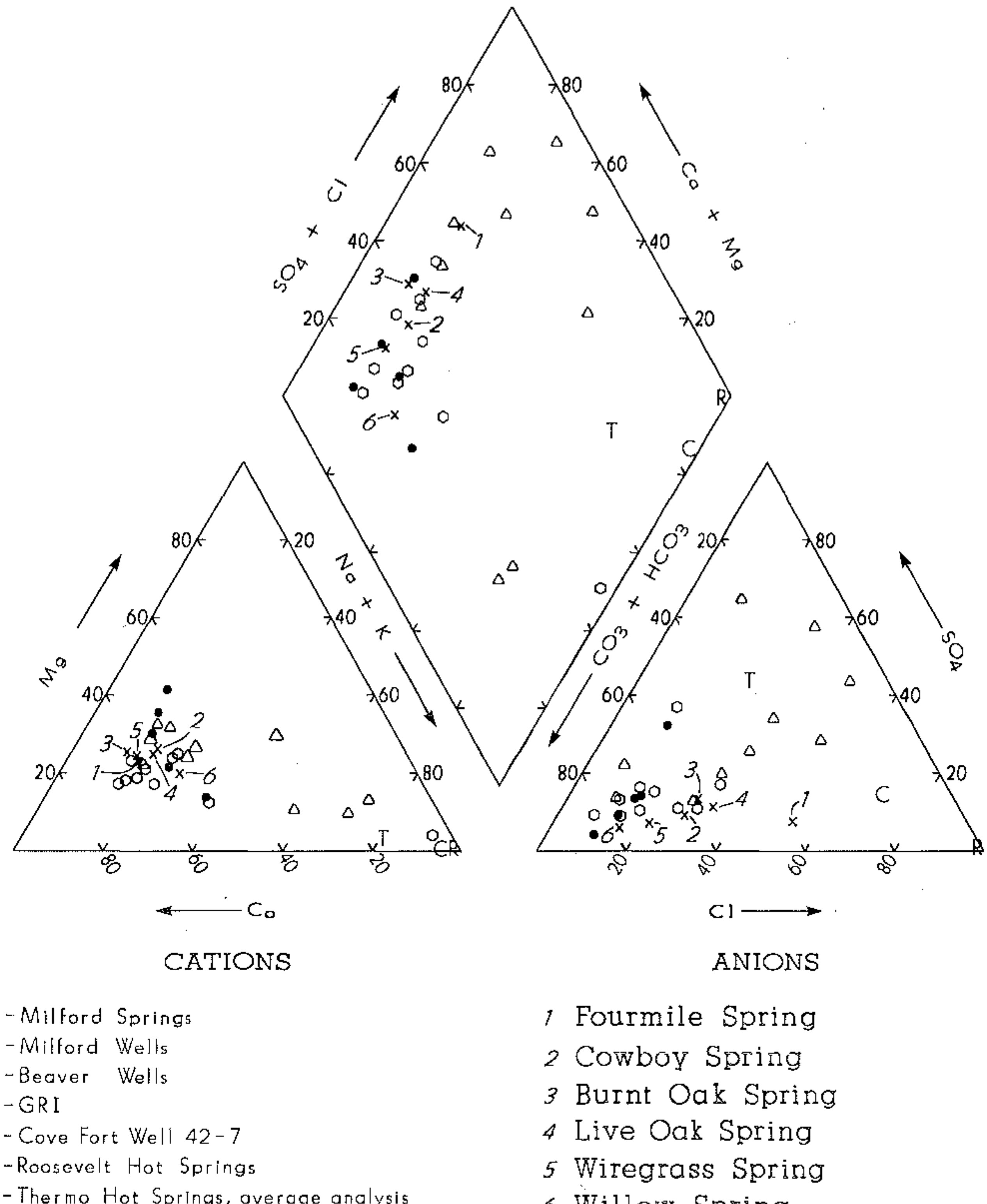

Figure 4. Trilinear diagram of GRI lease area water samples, selected thermal fluids, and cold waters from Milford and Beaver Valleys

meter temperature is from Live Oak Spring (#4). The relatively high K content of this water may be due to its flow through an altered zone near the syenite-granite contact. Willow Spring (#6) also has relatively high cation geothermometers, and the highest silica geothermometers of the sampled waters. Willow Spring is outside the GRI lease area, and flows from a lower elevation. It therefore may have been heated slightly more, or may just have a longer flowpath, and therefore more time for reaction with the surrounding rocks.

Comparison with Waters in Surrounding Areas

The GRI lease area is located between the Roosevelt Hot Springs and Cove Fort high-temperature geothermal areas. It is, however, approximately 1000 feet higher than either of these areas. Groundwater contours for the GRI lease area suggest that it is a zone of regional recharge at least to shallow aquifers in Beaver Valley (Mower, 1978). It should be noted, however, that Mower's contours in the lease area are based on extrapolation following topography; no data points exist in the lease.

Figure 4 also compares spring waters sampled from the lease area with shallow groundwaters in Beaver Valley (Mower, 1978) and Milford Valley (Mower and Cordova, 1974). The data selected for plotting the points on Figure 4 are listed in Table 4. The samples plotted from Beaver and Milford Valleys were selected to be closest to the GRI lease area, and those which qualitatively appeared to be representative of the groundwaters. Figure 4 illustrates that waters sampled from the GRI area are typical of the shallow, cool water in the region.

The GRI waters do not plot on the part of the trilinear diagram where Roosevelt Hot Springs (Mower and Cordova, 1974), Thermo Hot Springs (Klauk and Gourley, 1983), and Cove Fort (Ash et al., 1979) waters plot. Capuano and

TABLE 4

CHEMICAL ANALYSES USED FOR TRILINEAR PLOTS

Beaver Valley, Cold Wells (Mower, 1978)

Well #	Na	K	Ca	Mg	SiO_2	SO_4	Cl	HCO_3
C-28-7 15 BBA-2	19	2.1	60	11	29	27	47	164
C-29-7 3 CAB-1	12	1.6	39	6.4	27	25	34	88
C-29-7 11 CDA-1	21	1.9	52	9.9	27	30	15	188
C-29-7 19 BCD-1	40	7.0	46	9.7	45	45	22	199
C-29-7 21 CAC-1	15	3.5	56	10	28	30	31	180
C-29-7 21 CDB-S1	12	2.9	36	7.3	32	15	7.5	144
C-29-7 22 BDA-1	13	1.9	52	11	27	25	16	180
C-29-7 32 DBD-1	32	5.3	72	18	53	46	41	255
C-29-8 20 DCB-1	21	3.2	51	12	32	30	38	175
C-29-8 23 CAA-1	240	8.6	13	5.5	57	220	35	380

Milford Valley, Cold Wells (Mower and Cordova, 1974)

Well #	Na	K	Ca	Mg	SiO_2	SO_4	Cl	HCO_3
C-25-9 29 cbd-1	23	5.7	58	22	74	41	53	200
C-27-10 31 dcb-1	74	8.4	20	6.4	70	31	17	220
C-28-10 5 dad-2	510	8.1	310	200	n.d.	1,500	670	270
C-28-10 7 adb-1	62	2.8	13	5.8	35	40	16	160
C-28-10 8 aad-2	36	3.2	71	22	38	110	80	133
C-28-10 17 ccc-1	400	11	520	180	n.d.	1,200	1,000	293
C-29-10 5 add-1	39	4.5	120	37	37	140	180	142
C-29-10 5 cdd-4	30	4.7	120	26	n.d.	110	92	240
C-29-10 8 ddd-2	35	4.0	110	30	30	120	99	217
C-29-10 18 daa-1	16	3.0	51	11	33	41	38	141
C-30-9 7 adb-1	180	27	100	24	24	480	68	205

Milford Valley, Springs (Mower and Cordova, 1974)

Well #	Na	K	Ca	Mg	SiO_2	SO_4	Cl	HCO_3
C-28-9 14 dbb-S1	12	1.3	18	3.4	23	7.6	8	80
C-28-9 23 cdd-S1	5.5	1.1	13	2.9	11	8.6	5	51
C-28-9 29 cad-S1	21	1.9	67	20	17	19	18	306
C-29-9 17 bcb-S1	39	2.0	100	58	23	200	46	388
C-29-9 19 bbb-S1	18	2.6	67	29	21	45	37	284

<u>Thermal Springs and Wells</u>

	Na	K	Ca	Mg	SiO_2	SO_4	Cl	HCO_3	TDS
Cove Fort (Ash et al., 1979)	1310	585	32	4.8	170	560	1820	778	4775
Roosevelt Hot Springs (Mower and Cordova, 1974)	2100	470	19	3.3	400	65	3800	42	6940
Thermo Hot Springs (Klauk and Gourley, 1983)	371	50	69	10	84	460	222	401	1495

* n.d. = not determined

Cole (1982) suggest that adjustments for flashing and scaling indicate that a TDS value of slightly less than 10,000 is probably typical for Roosevelt Hot Springs deep thermal fluids. The analysis from Cove Fort is from Well 42-7, which is closest to Sulphurdale, where a high temperature system has been discovered. Well 42-7 may, however, have some contamination from drilling fluids.

The topographic elevation and chemistry of waters suggest that the GRI lease area is one of shallow recharge to groundwater aquifers. No data were uncovered in this study to indicate the presence of deeper thermal fluids.

ELECTRICAL RESISTIVITY SURVEY

Introduction

The exploration program proposed by ESL included a dipole-dipole electrical resistivity survey and a numerical model interpretation of the resulting data. The optimum location of survey lines within the GRI lease area was judged to be along a road which trends roughly north-south in Fortuna Canyon and along a northeast-trending road south of Fourmile Spring. The line locations are shown on Plate II. An electrode separation (a) of 1000 feet was used for both lines GRI-1 and GRI-2. Dipole-dipole lines with an electrode separation of 1000 feet have been used effectively in the delineation of near surface portions of the Roosevelt Hot Springs and Cove Fort-Sulphurdale geothermal systems (Ross et al., 1982a; Ross et al., 1982b).

The field survey was completed between October 1-4, 1984. A P-15C engine generator provided 120 volt 400 Hz input power to the Elliot Model 15A time domain transmitter. The maximum output power of the transmitter is 1500 watts, with a maximum output current of 5 amps. The transmitted waveform was 2 seconds on, 2 seconds off, 2 seconds reversed, 2 seconds off. A Fluke Model 8050A digital multimeter was used as a receiver. The Fluke multimeter has a reading precision greater than 0.01 mv of signal strength. The observed voltage was determined by the average of many (6 to 16) individual voltage readings, the number depending on noise level and signal strength. Observed voltages ranged from 1 mv to 200 mv. The transmitted current was monitored continuously and recorded by the transmitter operator. The apparent resistivity was calculated from the relation

$$\rho_a = \frac{\Delta V}{I} Q$$

where ΔV is the observed voltage, I is the transmitted current and Q is the geometric factor which includes unit conversion constants and increases for increasing separations (increasing n).

Line 1 trends north along Fortuna Canyon and over the divide to Cowbow Springs. Input currents for the transmitting dipoles varied from 2.9 to 4.0 amp and relatively strong signals were observed throughout the line. The observed data are shown in standard pseudosection format in Figure 5. The observed apparent resistivities are quite high and range from 110 ohm-m on the south to 400 ohm-m on the north. Apparent resistivities generally increase with increasing separation (increasing depth), and indicate a relatively simple resistivity structure. Resistivity values are generally accurate within 3% for line 1.

Line 2 trends northeast across the southern portion of the GRI lease. Apparent resistivities as low as 30 ohm-m were observed on the northeast (Figure 6) and increase irregularly to the southwest. Low apparent resistivities are noted at larger separations on the western portion of the line. Input currents remained high (3-5 amp) but signal strengths were lower than observed on most of line 1, and resistivity values are generally accurate within 5 percent.

Numerical Model Interpretation

The observed apparent resistivity data have been interpreted using a forward calculation numerical modeling routine, program IP2D (Killpack and Hohmann, 1979). Program IP2D assumes a two-dimensional geometry perpendicular to the resistivity line. A preliminary estimate of the resistivity distribution is input to the program, apparent resistivity values are computed using a finite-element algorithm and these computed resistivity values are

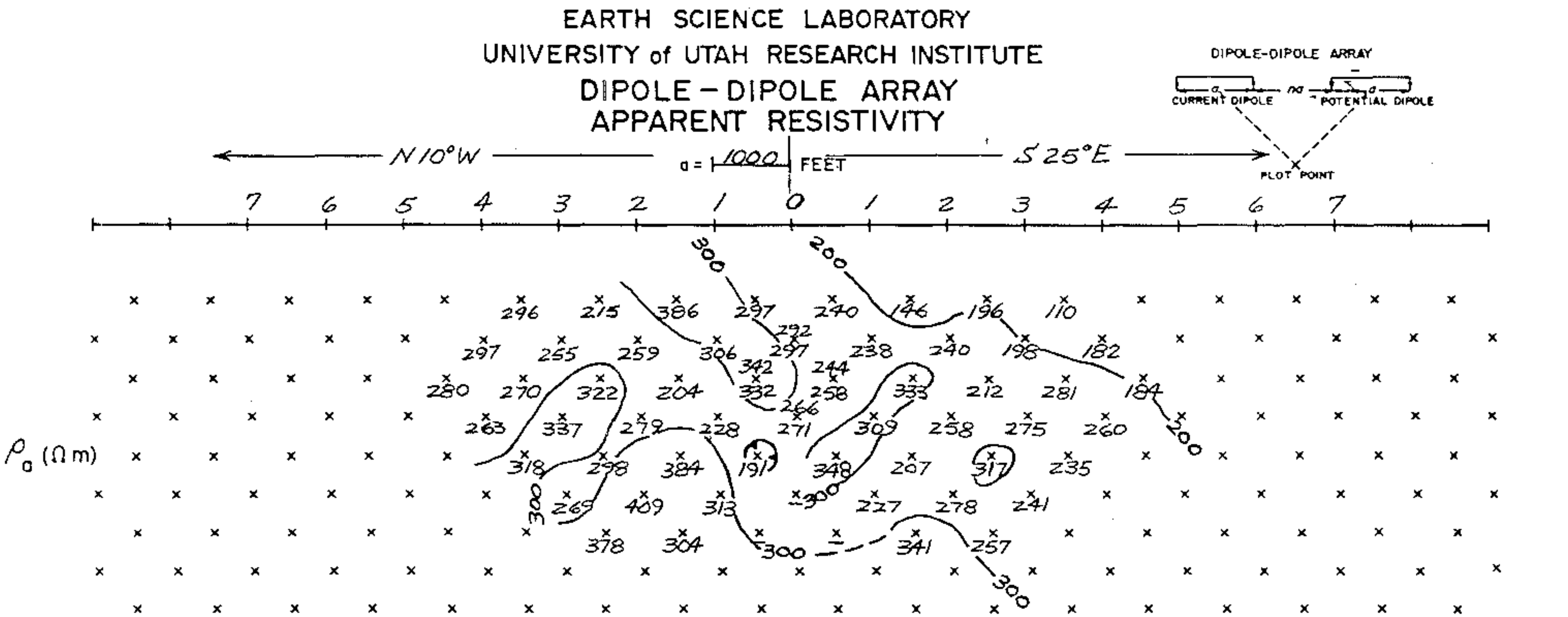

Figure 5. Observed electrical resistivity data, line GRI-1.

AREA Beaver Valley STATE Utah LINE GRI-1 DATA BY HPR/CEM DATE 10/2/84 TRANSMITTER Elliot-15A RECEIVER Fluke 8050A

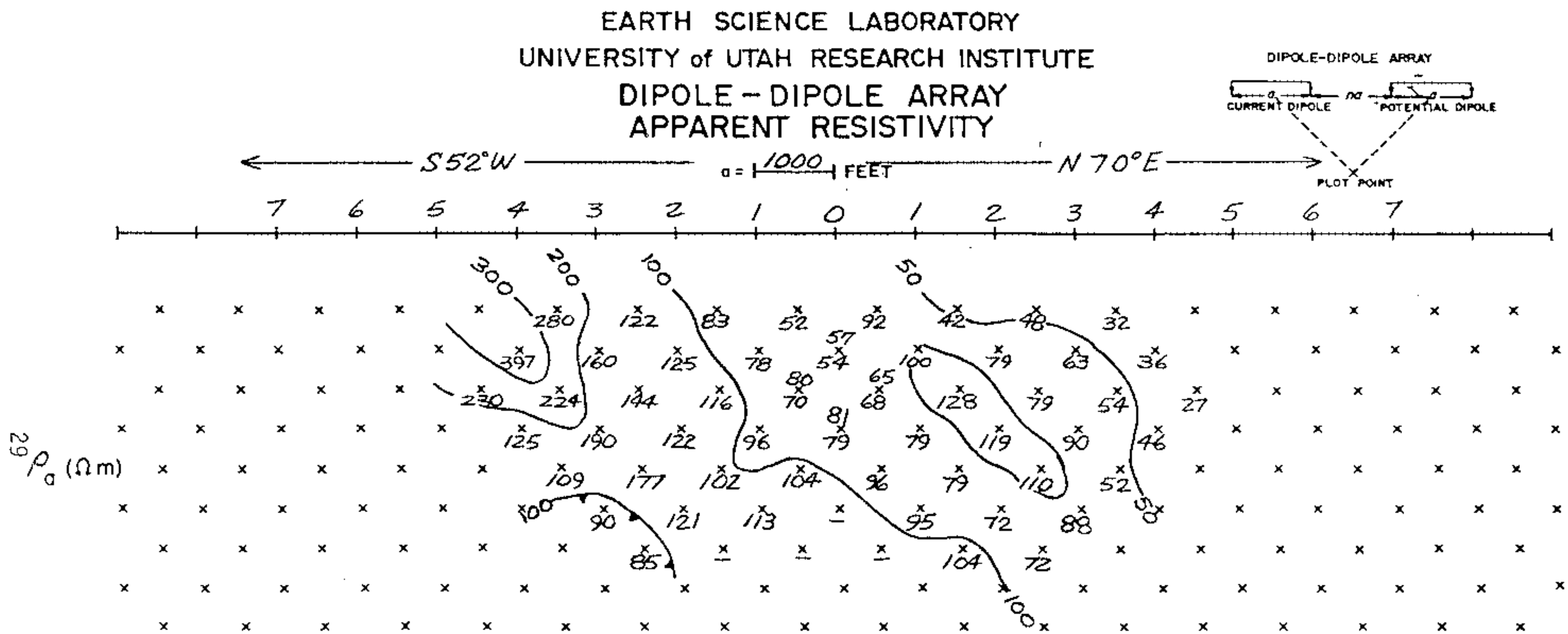

Figure 6. Observed electrical resistivity data, line GRI-2.

AREA Beaver Valley STATE Utah LINE GRI-2 DATA BY HPR/CEM DATE 10/3/84 TRANSMITTER Elliot-15A RECEIVER Fluke 8050A manually compared to the observed data. The model is changed through a series of iterations until a resistivity distribution is determined which produces a satisfactory agreement between observed and computed values.

Figure 7 shows the best fit model solution for line GRI-1 at an approximate true scale of 2000 ft per inch. A point by point comparison of observed and computed resistivity values is included in Appendix I. The intrinsic electrical resistivities of the geologic units, as interpreted through the numerical modeling process, are uniformly high at 100 to 400 ohm-m. The relatively thin zone of 100-200 ohm-m resistivity generally coincides with the outcrop area of Bullion Canyon volcanics. Higher resistivities, 200-400 ohm-m, are associated with the syenite intrusive to the north. The model solution indicates that no substantial zone of low resistivity is present within the 2500-3000 feet depths to which the observed data are sensitive. The resistivity distribution is presented in plan view for comparison to the geology in Figure 9.

Figure 8 shows a much wider ranging and complex resistivity distribution for GRI-2. Relatively low resistivities (25 ohm-m) occur east of station 2E for depths of a few hundred to perhaps 1000 feet near the eastern end of the line. This corresponds to rhyolite and rhyolite tuff of Gillies Hill. The 25 ohm-m resistivity is within but on the lower end of the general range for many other young rhyolitic units in the western United States. This may indicate somewhat more extensive alteration or higher than average porosity. The 25 ohm-m resistivities terminate abruptly near station 2, suggesting either a geologic structure or steeply dipping bedding.

Moderate (50 ohm-m) near-surface resistivities continue west to approximately station 2.5W but the thickness of the 50 ohm-m resistivity body varies

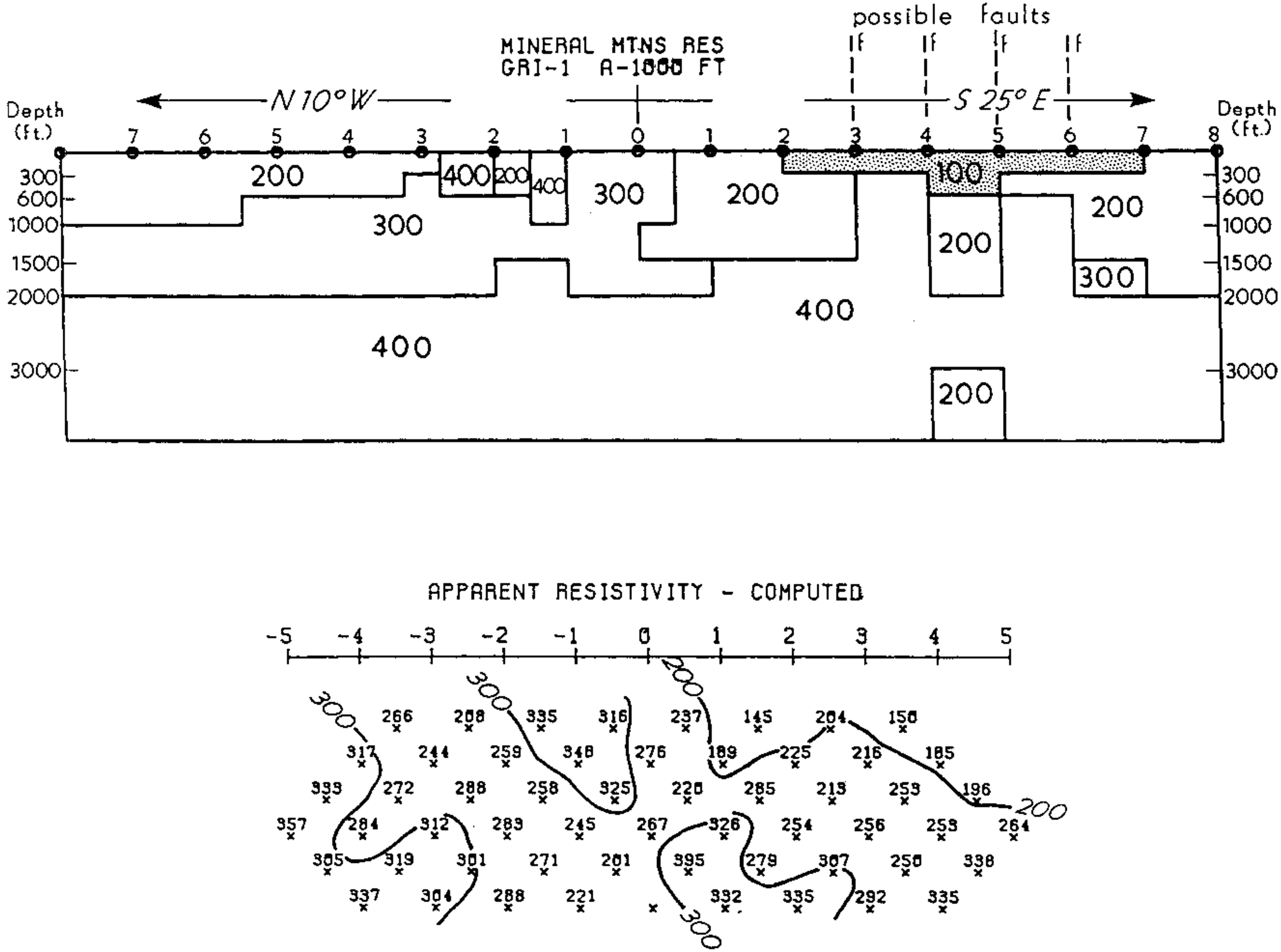

Figure 7. Numerical model solution, Line GRI-1.

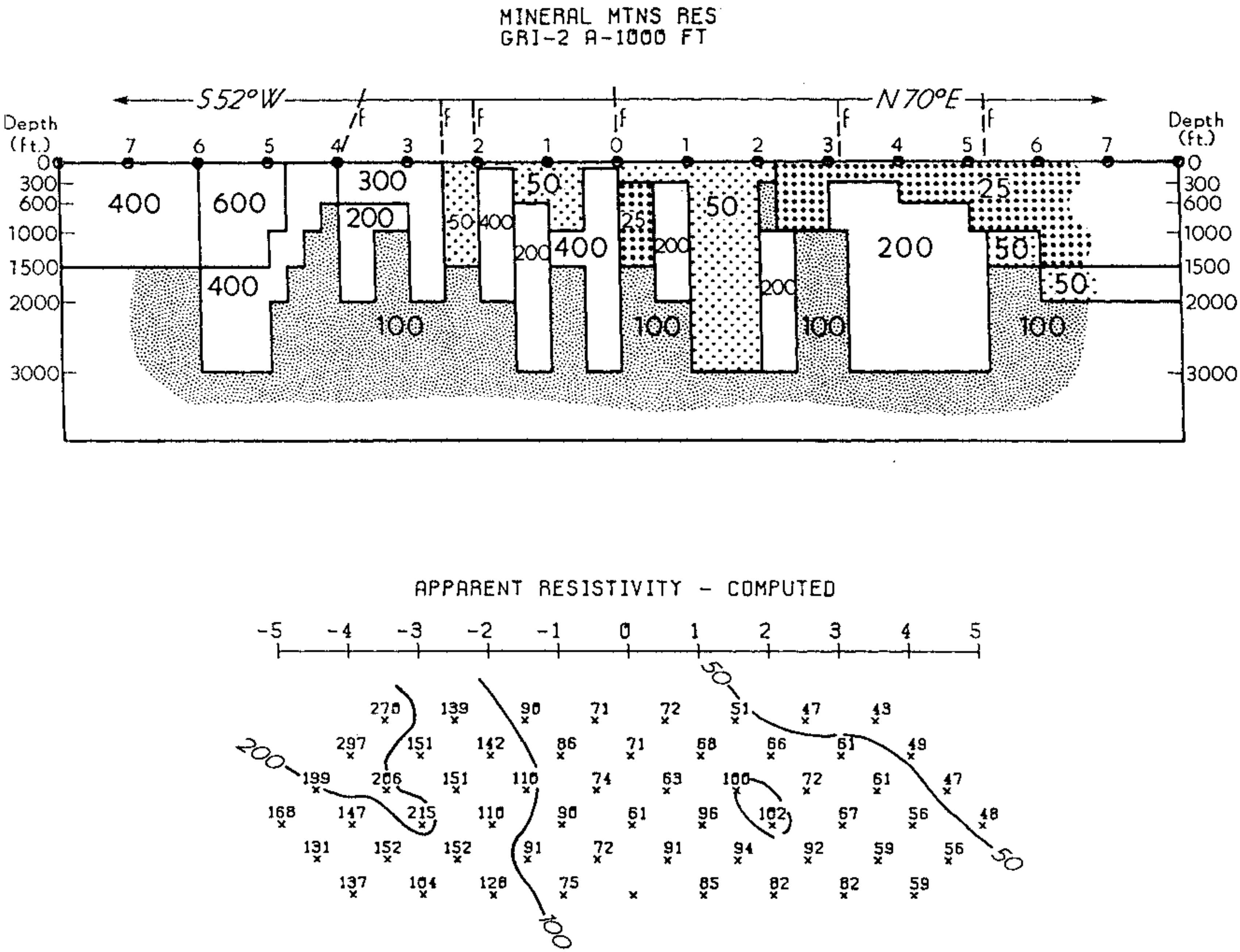

Figure 8. Numerical model solution, Line GRI-2.

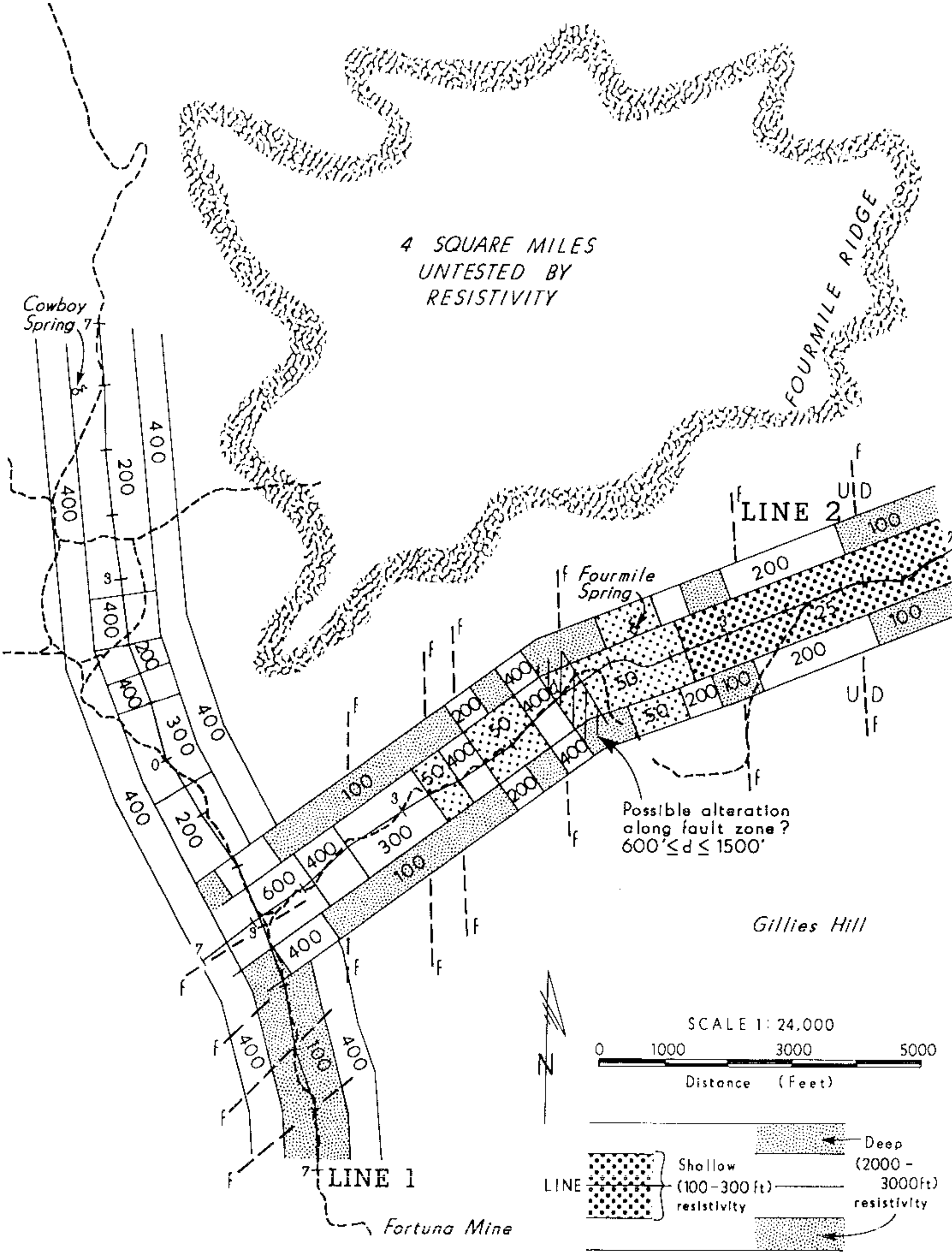

Figure 9. Interpreted electrical resistivity distribution along lines GRI-1 and GRI-2.

considerably. A narrow zone of 25 ohm-m resistivity extends from about 300 to 1500 feet deep between station 0 and 0.5E, perhaps indicating increased porosity and/or alteration along a mapped fault. A major resistivity discontinuity occurs at approximately station 2.5W where a 50 ohm-m unit is juxtaposed against 300 ohm-m within an area where Bullion Canyon volcanics crop out, and near the projection of a north-trending fault. The geometry of the resistivity distribution suggests the presence of several north-trending structures (or other lithologic changes) at depths of 100-1000 feet between stations 2.5W and 2.5E. This could be the expression of the western border of the deeper part of the Cove Fort-Beaver graben. The numerical model interpretation and the observed data are fairly accurate to depths of about 2000-2500 feet. The best-fit model solution indicates a relatively broad zone of 100 ohm-m resistivity at these depths, but the 100 ohm-m resistivities could actually be north or south of the line at somewhat reduced depths.

There is no real indication of the low (4-10 ohm-m) resistivity zones seen at Roosevelt Hot Springs and Cove Fort-Sulphurdale. A single narrow zone of 25 ohm-m near a fault at station 0 could possibly indicate increased fracturing or alteration along the structure, or could arise from a steeply-dipping low resistivity tuff unit. Approximately 28,000 line feet (5.3 line miles) of resistivity data were obtained along two profiles in this survey. The lines followed existing roads in the western and south-central portion of the GRI lease block and did not detect a substantial zone of low resistivities which could be attributed to a geothermal occurrence within 2500 feet of the surface along these lines. Low resistivity zones more than 1000 feet from the lines and at a depth of more than 1000 feet would not necessarily have been detected. Thus, an area of approximately four square miles in the northeastern portion of the GRI lease block remains untested by the present survey.

COMPARISON OF GRI LEASE AREA WITH COVE FORT AND ROOSEVELT HOT SPRINGS KNOWN GEOTHERMAL RESOURCE AREAS (KGRAs)

The study area has strong similarities to the nearby KGRAs in lithologies and structures. The lease area is on the east margin of the Mineral Mountains pluton; Roosevelt Hot Springs is along the west margin of the pluton. North-south normal faults and narrow grabens are present in both locations. The Bullion Canyon Volcanics and younger volcanic rocks overlie Paleozoic sedimentary rocks as in the Cove Fort area, however the Paleozoic rocks are probably much more limited in the study area. Late Tertiary, low-angle faulting has occurred in the lease area and in both KGRAs. However, the exposed extent of this faulting is limited in the study area, and it is not known to extend to great depth. In the Roosevelt Hot Springs and Cove Fort KGRAs, low-angle faulting at depth provides fracture reservoirs and structural control for the geothermal systems (Nielson and Moore, 1979). Quaternary basaltic rocks, less than one million years old, are present just west of the lease block and extend northeast to the Cove Fort area. More quartz veins and alteration of bedrock are exposed in the lease area than in the neighboring KGRAs.

The lack of thermal springs, sinter or recently altered alluvium in the GRI lease are dissimilar to the KGRAs. The lease area is located on a topographic high and probably a groundwater recharge area whereas both Roosevelt Hot Springs and Cove Fort are at the foot of mountain ranges, adjacent to alluvial filled valleys. The lease block is up the hydrologic gradient from Roosevelt Hot Springs (Ross et al., 1982a) and probably up the hydrologic gradient from the Roosevelt heat source below the Quaternary rhyolite domes. While some of these comparisons appear unfavorable, it should be noted that the blind Desert Peak system in Nevada occurs under a topographic high next to Bailey Hot Springs.

A low resistivity zone similar to those at Roosevelt Hot Springs and Cove Fort was not detected by the limited dipole-dipole survey in the lease block but the possibility remains of a geothermal system at greater depth or in areas not covered by the survey.

RECOMMENDATIONS

The structures and lithologies present in the northeastern four square miles of the lease block are sufficiently encouraging to recommend drill testing or additional geophysical surveys which may be cost effective in siting a deep thermal gradient test as a possible next step to evaluate the lease block. Two survey types should be considered.

A. Bipole-dipole with follow-up dipole-dipole

Two long bipole (2000-3000 ft) transmitters with perpendicular receiver legs 5000-8000 feet distant could quite effectively cover four to six square miles in the Fourmile Canyon-Woodtick Hill area, to depths of about 3000-4000 feet. Any specific zone of low apparent resistivity would be crossed by a single dipole-dipole line to provide depth information and lateral resolution. The cost is estimated at $6500-$9500.

B. AMT or CSMAT Survey

An audiomagnetotelluric (AMT) survey, perhaps using a controlled current source (CSAMT) and reading to low frequencies of 0.5-1.0 Hz could also provide the desired resistivity information, perhaps to depths of 4000 feet, at a somewhat higher cost. A rough cost estimate would be $10,000-$15,000 depending on the use of a controlled source, number of stations, noise levels, and other factors.

Although the present resistivity survey did not detect a fracture or porous geothermal reservoir, thermal fluid could be present in a fault zone too narrow to be resolved by the survey. Also significant structures are present in the northeast four square miles which are untested by electrical surveys.

Considering the high elevation of the lease area compared to Sulphurdale, an intermediate thermal gradient hole to about 2000 feet would be needed to determine if there is an anomalous thermal gradient at depth. If thermal gradient drilling is undertaken to evaluate further the property, three possible areas are suggested based on structural setting. These locations are: 1) the narrow graben in Section 6, T27S, R7W., where faults, alteration and quartz veins indicate a significant structure; 2) the narrow graben in the NE 1/4, Sec. 7, T27S, R7W, for the same reasons as above; 3) Fourmile Canyon in Section 5, T27S, R7W, where recent movement has occurred along the fault which bounds the east side of the canyon and trends north to the Cove Fort cinder cone. The proposed bipole-dipole survey may give a better indication of drilling targets.

REFERENCES CITED

Aleinikoff, J. N., Nielson, D. L., Hedge, C. E., and Evans, S. H., Jr., in press, Geochronology of Precambrian and Tertiary rocks in the Mineral Mountains, south-central Utah, in Shorter Contributions to Isotope Research: U.S. Geol. Survey Prof. Paper.

Ash, D. L., Dondanville, R. F., and Gulati, M. S., 1979, Geothermal reservoir assessment, Cove Fort/Sulphurdale Unit, final report for the period September, 1977 - July, 1979: Union Oil Company, U.S. Department of Energy Contract DE-AC08-77ET-28405, 34 p.

Best, M. G., McKee, E. H., and Damon, P. E., 1980, Space-time-composition patterns of Late Cenozoic mafic volcanism, southwestern Utah and adjoining areas: Am. Jour. Sci., v. 280, p. 1035-1050.

Capuano, R. M., and Cole, D. R., 1982, Fluid-mineral equilibria in a hydrothermal system, Roosevelt Hot Springs, Utah: Geochem. Cosmochim. Acta, v. 46, p. 1353-1364.

Crecraft, H. R., Nash, W. P., and Evans, S. H., Jr., 1981, Late Cenozoic volcanism at Twin Peaks, Utah: geology and petrology: Jour. Geophy. Research, v. 86, no.B11, p. 10303-10320.

DiPippo, R., 1984, Geothermal power development, 1984 overview and update: Geothm. Res. Council, Bull., v. 13, no. 9, p. 3-12.

Evans, S. H., Jr., and Nielson, D. L., 1982, Thermal and tectonic history of the Mineral Mountains intrusive complex: Geothm. Res. Council, Transactions, v. 6, p. 15-18.

Evans, S. H., Jr., and Steven, T. A., 1982, Rhyolites in the Gillies Hill-Woodtick Hill area, Beaver County, Utah: Geol. Soc. Am., Bull. v. 93, p. 1131-1141.

Fournier, R. O., 1981, Application of water chemistry to geothermal exploration and reservoir engineering, in Rybach, L. and Muffler, L.J.P.: Geothermal Systems: Principles and Case Histories: John Wiley and Sons, N.Y., p. 109-144.

Fournier, R. O., and Potter, R. W. II, 1979, Magnesium correction to the Na-K-Ca chemical geothermometer: Geochim. Cosmochim. Acta, v. 43, p. 1543-1550.

Fournier, R. O., and Truesdell, A. H., 1974, Geochemical indicators of subsurface temperature - Part 2, Estimation of temperature and fraction of hot water mixed with cold water: U.S. Geol. Survey, Jour. Research, v. 2, p. 263-270.

Hem, J. D., 1970, Study and interpretation of the chemical characteristics of natural water: U.S. Geol. Survey Water-Supply Paper 1473, 363 p.

Hoover, J. D., 1974, Periodic Quaternary volcanism in the Black Rock Desert, Utah: Brigham Young Univ. Geol. Studies, v.. 21, p. 2-72.

Killpack, T. J., and Hohmann, G. W., 1979, Interactive dipole-dipole resistivity and IP modeling of arbitrary two-dimensional structures: Univ. Utah Research Inst., Earth Science Lab., Rept. 15, 114 p.

Klauk, R. H., and Gourley, C., 1983, Geothermal assessment of a portion of the Escalante Valley, Utah: Utah Geol. Min. Survey, Special Study 63, 57 p.

Kroneman, R. L., 1981, Guide to water sampling: Univ. Utah Research Inst., Earth Science Lab., unpub. ms., 10 p.

Lipman, P. W., Rowley, P. D., Mehnert, H. H., Evans, S. H., Jr., Nash, W. P., and Brown, F. H., 1978, Pleistocene rhyolite of the Mineral Mountains, Utah-geothermal and archeological significance: U.S. Geol. Survey, Jour. Research, v. 6, p. 133-147.

Mabey, D. R., Zietz, I., Eaton, G. P., and Kleinkopf, M. D., 1978, Regional magnetic patterns in part of the Cordillera in the western United States, in R. B. Smith and G. P. Eaton, eds., Cenozoic tectonics and regional geophysics of the western Cordillera: Geol. Soc. America Mem. 152, p. 313-340.

Machette, M. N., and Steven, T. A., 1983, Geologic map of the northwest quarter of the Beaver Quadrangle, Beaver County, Utah: U.S. Geol. Survey, Misc. Invest. Map 1-1445.

Moore, J. N., and Samberg, S. M., 1979, Geology of the Cove Fort-Sulphurdale KGRA: Univ. Utah. Research Inst., Earth Science Lab., Rept. 18, 44 p.

Mower, R. W., 1978, Hydrology of the Beaver Valley area, Beaver County, Utah, with emphasis on groundwater: Utah Department of Water Resources, Technical Publication 63, 90 p.

Mower, R. W., and Cordova, R. M., 1974, Water resources of the Milford area, Utah, with emphasis on groundwater: Utah Department of Natural Resources, Technical Publication 43, 106 p.

Nielson, D. L., Sibbett, B. S., McKinney, D. B., Hulen, J. B., Moore, J. N., and Samberg, S. M., 1978, Geology of Roosevelt Hot Springs KGRA, Beaver County, Utah: Univ. Utah Research Inst., Earth Science Lab., Rept. 12, 120 p.

Nielson, D. L., and Moore, J. N., 1979, The exploration significance of low-angle faults in the Roosevelt Hot Springs and Cove Fort-Sulphurdale Geothermal System, Utah: Geothm. Res. Council, Transactions, v. 3, p. 503-506.

Ross, H. P., Nielson, D. L., and Moore, J. N., 1982a, Roosevelt Hot Springs Geothermal System, Utah - case study: Am. Assoc. Petrol. Geol. Bull., v. 66, no. 7, p. 879-902.

Ross, H. P., Moore, J. N., and Christensen, O. D., 1982b, The Cove Fort-Sulphurdale KGRA - A geologic and geophysical case study: Univ. Utah Research Inst., Earth Science Lab., Rept. 90, 32 p.

Rowley, P. D., Steven, T. A., Anderson, J. J., and Cunningham, C. G., 1979, Cenozoic stratigraphic and structural framework of southwestern Utah; U.S. Geol. Survey, Prof. Paper 1149, 22 p.

Sibbett, B. S., and Nielson, D. L., 1980, Geology of the Central Mineral Mountains, Beaver County, Utah: Univ. Utah Research Inst., Earth Science Lab. Report 33, 42 p.

APPENDIX I

NUMERICAL MODEL OUTPUT

GRI Lease Area
East Mineral Mountains, Utah

Resistivity Line GRI-1, a = 1000 feet: Final Solution

Resistivity Line GRI-2, a = 1000 feet: Final Solution

```
MINERAL MTNS RESISTIVITY
GRI-1  A-1000 FT
MEDIA RESISTIVITY (OHM-METERS)
        25.00      50.00     100.00     200.00     300.00
       400.00     600.00
MEDIA PFE (%)
         0.00       0.00       0.00       0.00       0.00
         0.00       0.00
```

```
 88  77  66  55  44  33  22  11  00  11  22  33  44  55  66  77  88     Depth (ft.)
......1.........2.........3.........4.........5.........6.........7
4444444444444444444446664466555555444444333333333333333333334444444   100
4444444444444444444446664466555555444444333333333333333333334444444   300
4444444444444444444556664466555555444444444466663333444444444444444   600
4444444444555555555555555566555555444444444466664444666644444444444   1000
5555555555555555555555555555555544444444444466664444666644444444444   1500
5555555555555555555555556666555555556666666666664444666655554444444   2000
6666666666666666666666666666666666666666666666666666666666666666666   3000
6666666666666666666666666666666666666666666666664444666666666666666   4000
6666666666666666666666666666666666666666666666666666666666666666666
6666666666666666666666666666666666666666666666666666666666666666666
6666666666666666666666666666666666666666666666666666666666666666666
......1.........2.........3.........4.........5.........6.........7
```

APPARENT RESISTIVITY (CALCULATED)

```
 -5     -4     -3     -2     -1      0     +1     +2     +3     +4     +5
  :------:------:------:------:------:------:------:------:------:------:

                                                             observed
                                                             calculated
          296    215    386    297     240    146    196    110
          266.   208.   335.   316.    237.   145.   204.   150.

       297    255    259    306    295    238    240    198    182
       317.   244.   259.   348.   276.   189.   225.   216.   185.

    280    270    322    204    337    251    333    212    281    184
    333.   272.   288.   258.   325.   220.   285.   213.   253.   196.

        263    337    279    228    268    309    258    275    260
 357.   284.   312.   283.   245.   267.   326.   254.   256.   253.   264.

           318    298    384    191    348    207    317    235
    305.   319.   301.   271.   201.   395.   279.   307.   250.   338.

               269    409    313           227    278    241
       337.    304.   288.   221.          332.   335.   292.   335.

               378    304                         341    257
```

Resistivity Line GRI-1, a=1000 feet: FINAL SOLUTION

Iter #10
File #16

```
MINERAL MTNS RESISTIVITY
GRI-2 A-1000 FT
MEDIA RESISTIVITY (OHM-METERS)
        25.00       50.00     100.00     200.00     300.00
       400.00      600.00
MEDIA PFE (%)
         0.00        0.00       0.00       0.00       0.00
         0.00        0.00

  88  77  66  55  44  33  22  11  00  11  22  33  44  55  66  77  88   Depth
.........1.........2.........3.........4.........5.........6.........7  (ft)
66666666666777776665555552222222222222222222111111111111111111111111111 -100
66666666666777776665555552266222266222222222111111111111111111111111111 -300
66666666666777776665555552266222266114422223111444411111111111111111111 -600
66666666666777776634444552266442266114422223111444444441111111111111111 -1000
66666666666777766334433552266446666114422224433344444444422211111111111 -1500
33333333333666663334433553366443366334422224433344444444433322222222222 -2000
33333333333666633333333333333443366333322224433344444444433333333333333 -3000
33333333333333333333333333333333333333333333333333333333333333333333333 -4000
33333333333333333333333333333333333333333333333333333333333333333333333
33333333333333333333333333333333333333333333333333333333333333333333333
33333333333333333333333333333333333333333333333333333333333333333333333
.........1.........2.........3.........4.........5.........6.........7
```

APPARENT RESISTIVITY (CALCULATED)

```
 -5      -4      -3      -2      -1       0      +1      +2      +3      +4      +5
  :-------:-------:-------:-------:-------:-------:-------:-------:-------:-------:

                                                                           observed
              280     122     83      52        92      42      48      32
              270.    139.    90.     71.       72.     51.     47.     43.  calculated

          397     160     125     78      56      100     79      63      36
          297.    151.    142.    86.     71.     68.     66.     61.     49.

      230     224     144     116     75        67      128     79      54      27
      199.    206.    151.    110.    74.       63.     100.    72.     61.     47.

  168.    125     190     122     96      80      79      119     90      46
          147.    215.    110.    90.     61.     96.     102.    67.     56.     48.

      131.    109     177     102     104       96      79      110     52
              152.    152.    91.     72.       91.     94.     92.     59.     56.

          137.    90      121     113               95      72      88
                  104.    128.    75.               85.     82.     82.     59.

                  85      -                                 104     72
```

Resistivity Line GRI-2, a=1000 feet: FINAL SOLUTION